International Journal of Thermal Sciences 52 (2012) 73–82

Contents lists available at SciVerse ScienceDirect

International Journal of Thermal Sciences

journal homepage: www.elsevier.com/locate/ijts

A general analytical solution for heat conduction in cylindrical multilayer composite laminates

M.H. Kayhani, M. Norouzi, A. Amiri Delouei*

Mechanical Engineering Department, Shahrood University of Technology, Shahrood, Semnan 361 9995161, Iran

ARTICLE INFO

Article history:
Received 9 November 2010
Received in revised form
1 September 2011
Accepted 2 September 2011
Available online 2 October 2011

Keywords:
Analytical solution
Composite laminate
Heat conduction
Cylinder
Fourier transformation

ABSTRACT

This paper presents a steady analytical solution for heat conduction in a cylindrical multilayer composite laminate in which the fiber direction may vary between layers. The analytical solution is obtained for general linear boundary conditions that are suitable for various conditions including combinations of conduction, convection, and radiation both inside and outside the cylinder. The Sturm–Liouville theorem is used to derive an appropriate Fourier transformation for this problem. The temperature distribution is obtained by applying this transformation to the governing equation. The coefficients of the solution are obtained by solving a set of equations generated by applying the boundary conditions inside and outside the cylinder, and the continuity of temperature and heat flux at boundaries between adjacent layers. The recursive Thomas algorithm is used to obtain the solution of this set of equations. The applicability of the current solution for a wide range of applied problems is confirmed by considering two industrial examples.

1. Introduction

Composite materials have been developed for a wide range of industrial applications, including piping, pressure vessels, fluid reservoirs, aerospace components, and naval structures. Composite materials have many favorable properties, including high strength-to-weight ratios and high corrosion resistances. Many studies have investigated the mechanical and thermomechanical properties of composite laminates [1–3]. However, few studies have considered heat conduction in these anisotropic materials. Heat conduction in composite laminates is particularly important for preventing thermal fracture, analyzing fiber placement in production processes, and controlling directional heat transfer through laminates by varying the angles of the fibers.

Most research in this field has been conducted on anisotropic crystals [4,5]. Ma and Chang [6] analytically investigated heat conduction in anisotropic multilayered media. They converted the anisotropic problem into a simple isotropic problem by performing a linear coordinate transformation. One application of composite materials is in the manufacture of superconducting materials. Cha et al. [7] found an analytical solution for one-dimensional transient heat conduction with a distributed heat source. This solution enabled the authors to predict the transverse temperature distribution and the heat generation rate per unit volume of the composite superconductor. They showed that the generation rate is directly proportional to the current in the stabilizer. Kulkarani and Brady [8] developed a mathematical model based on the volume percentages of matrix and fibers for heat transfer in laminated carbon–carbon composites. This model can estimate the heat transfer coefficients parallel and perpendicular to the fibers. Johansson and Lesnic [9] showed applications of the method of fundamental solution (MFS) for transient heat conduction in layered materials and extended this method to numerically estimate temperature fields in these materials. The MFS belongs to a class of methods known as boundary methods, and it is used to obtain the numerical solution of certain elliptic boundary value problems [10]. Sun and Wichman [11] presented a theoretical solution for transient heat transfer in a one-dimensional three-layer composite slab and compared the obtained results with the finite element solution. Karageorghis and Lesnic [12] introduced a solution for heat conduction in a laminated composite material whose conduction coefficient dependence on temperature and boundary conditions was based on convection and radiation. Haji-sheikh et al. [13] obtained a mathematical formulation for steady-state heat conduction and temperature distribution in multi-layer bodies. They found that the eigenvalues are real for homogeneous layers, but that they can be imaginary for orthotropic layers. Guo et al. [14] studied the temperature distribution in thick polymer matrix laminates and compared it with the numerical solution. They used the finite element method to solve transient heat transfer in polymer matrix composite laminates. They included the internal

* Corresponding author. Tel.: +98 9155333946; fax: +98 2733335445.
E-mail addresses: h_kayhani@shahroodut.ac.ir (M.H. Kayhani), mnorouzi@shahroodut.ac.ir (M. Norouzi), a.a.delouei@gmail.com (A. Amiri Delouei).

1290-0729/$ – see front matter © 2011 Elsevier Masson SAS. All rights reserved.
doi:10.1016/j.ijthermalsci.2011.09.002

energy generated by chemical reactions in the heat transfer equation. Singh et al. [15] obtained an analytical solution for conductive heat transfer in a multilayer composite in the radial direction of a polar coordinate system. Bahadur and Bar-Cohen [16] presented an analytical solution for the temperature distribution and the heat flux in a cylindrical fin with an orthotropic conduction coefficient and they compared the results with the finite element solution. Onyejekwe [17] obtained an exact analytical solution for conductive heat transfer in composite media using boundary integral theory.

Tarn and Wang [18,19] studied conductive heat transfer in cylinders made from a functional graded material and composite laminates. In addition, many studies have investigated conductive heat transfer in nanocomposite materials [20,21].

Kayhani et al. [22] analytically investigated conductive heat transfer in cylindrical composite laminates in the radial and angular directions (r,φ). The solution they obtained is only valid for composite pipes and vessels with a high ratio of longitudinal to radial dimensions, which is a special case of very long pipes and vessels.

The present paper presents an exact solution for conductive heat transfer in cylindrical composite laminates. This analytical solution can be used to analyze conductive heat transfer and thermal fracture in composite pipes and vessels. Fig. 1 shows the geometry of the composite laminate considered in this study. The fibers are wound around the cylinder and the direction of the fibers in each lamina can vary between layers. Unlike Kayhani et al. [22], we focus on axisymmetric heat transfer in cylindrical composite laminates by considering heat conduction in the longitudinal and radial directions (r,z). Here, we obtain a more complete solution by extending the solution of Kayhani et al. [23] through deriving recursive relations for the series coefficients and applying the most general linear boundary conditions for both pipes and solid cylinders. The main innovation of the present study is the derivation of the most general analytical solution based on complicated boundary conditions, which are based on combinations of conduction, convection, and radiation inside and outside the cylindrical laminate. For this purpose, we use the Sturm–Liouville theorem to derive an appropriate Fourier transformation. We then use this Fourier transformation to convert the partial differential equation for heat transfer in cylindrical composite laminates into an ordinary differential equation. Fourier coefficients are obtained by solving a set of equations consisting of thermal boundary conditions inside and outside the cylinder, and applying the continuity of temperature and heat flux between the layers. The Thomas algorithm is used to obtain the solution of the set of equations. This problem is solved for two examples of applications to demonstrate the ability of the current solution to obtain the temperature distributions in various industrial problems.

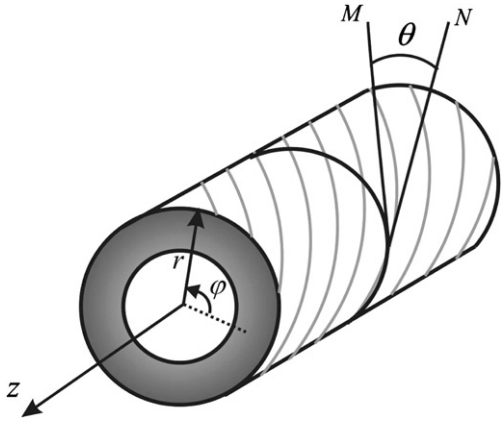

Fig. 1. Direction of fibers in a cylindrical laminate.

2. Conductive heat transfer in composites

The Fourier relation for conductive heat transfer in orthotropic materials in a cylindrical system is given by [24]:

$$\begin{Bmatrix} q_r \\ q_\varphi \\ q_z \end{Bmatrix} = -\begin{bmatrix} k_{11} & k_{12} & k_{13} \\ k_{21} & k_{22} & k_{23} \\ k_{31} & k_{32} & k_{33} \end{bmatrix} \begin{Bmatrix} \dfrac{\partial T}{\partial r} \\ \dfrac{1}{r}\dfrac{\partial T}{\partial \varphi} \\ \dfrac{\partial T}{\partial z} \end{Bmatrix} \tag{1}$$

where q is the heat flux, k_{ij} are the conductive heat transfer coefficients, and T is the temperature. According to thermodynamic reciprocity, the tensor of the conductive heat transfer coefficients should be symmetric:

$$k_{ij} = k_{ji}. \tag{2a}$$

According to the second law of thermodynamics, the diametric elements of this tensor are positive so that the following relation holds:

$$k_{ii}k_{jj} > k_{ij}^2 \quad \text{for: } i \neq j. \tag{2b}$$

From the Clausius–Duhem inequality, we obtain the following inequalities for the elements of the conductivity tensor of orthotropic materials [24–26]:

$$k_{(ii)} \geq 0 \tag{2c}$$

$$\frac{1}{2}\left(k_{(ii)}k_{(jj)} - k_{(ij)}k_{(ji)}\right) \geq 0 \tag{2d}$$

$$\varepsilon_{ijk}k_{(1j)}k_{(2j)}k_{(3j)} \geq 0 \tag{2e}$$

where $k_{(ij)}$ represents the symmetric part of the conductivity tensor:

$$k_{(ij)} \equiv k_{(ij)} = \frac{k_{ij} + k_{ji}}{2}. \tag{2f}$$

These relations are valid in all coordinate systems. Two different coordinate systems are generally used when considering problems in composite laminates: an on-axis coordinate system (x_1,x_2,x_3) and an off-axis coordinate system (r,ϕ,z) [27]. The directions of the on-axis coordinates depend on the fiber orientation: x_1 is parallel to the fibers, x_2 is perpendicular to the fiber in layer and x_3 is perpendicular to the layer. Composite laminates are generally fabricated by laying layers on top of each other. Since the fiber orientation may differ between laminas, we need to define an off-axis coordinate system to study the physical properties in specified directions. Thus, there is an angular deviation of θ between the on-axis and off-axis systems, and their coordinates are coincident. In the on-axis coordinate system, the Fourier equation for a composite material in a cylindrical system is given as follows [28]:

$$\begin{Bmatrix} q_r \\ q_\varphi \\ q_z \end{Bmatrix} = -\begin{bmatrix} k_{22} & 0 & 0 \\ 0 & k_{11} & 0 \\ 0 & 0 & k_{22} \end{bmatrix}_{\text{on}} \begin{Bmatrix} \dfrac{\partial T}{\partial r} \\ \dfrac{1}{r}\dfrac{\partial T}{\partial \varphi} \\ \dfrac{\partial T}{\partial z} \end{Bmatrix}. \tag{3}$$

The off-axis conductivity tensor $[\bar{k}]$ is obtained by applying the rotation θ to the on-axis conductivity tensor $[k]$:

$$[\bar{k}] = [T(\theta)][k][T(-\theta)] \tag{4}$$

where $T(\theta)$ is the rotation transformation:

$$T(\theta) = \begin{bmatrix} \cos\theta & -\sin\theta & 0 \\ \sin\theta & \cos\theta & 0 \\ 0 & 0 & 1 \end{bmatrix}. \quad (5)$$

The heat conduction coefficients can be obtained from experimental measurements on laminates parallel and perpendicular to the fibers. In the absence of experimental data, they can be calculated from theoretical models. Maxwell [29] first developed a theoretical model for two-phase systems, using potential theory to derive the effective thermal conductivity of randomly distributed, non-interacting spheres in a continuous matrix. Bruggeman [30] improved the Maxwell model by considering an infinite number of small additions to a homogeneous mixture of the two phases. In addition, some statistical analysis and bounding techniques have been applied to this problem [31,32]. Halpin [28] presented the following relations:

$$k_{11} = \upsilon_f k_f + \upsilon_m k_m \quad (6a)$$

$$k_{22} = k_m \frac{1+\varsigma\eta\upsilon_f}{1-\eta\upsilon_f} \quad (6b)$$

where k_f and k_m are respectively the heat conduction coefficients of the fibers and the matrices, and υ_f and υ_m are respectively the volume percentages of the fibers and the matrices. In addition, η and ς are expressed as follows:

$$\eta = \frac{k_f/k_m - 1}{k_f/k_m + \varsigma} \quad (6c)$$

$$\varsigma = {}^{1}/_{(4-3\upsilon_m)}. \quad (6d)$$

Lewis and Nielson [33] incorporated the particle shape and packing orientation for a two-phase system. Another important parameter that needs to be considered is the thermal contact resistance (TCR). The TCR significantly affects the effective thermal conductivity of composites, but it is very difficult to determine its value [34]. Macedo and Ferreira [35] investigated the TCR values of polymer-based carbon fibers, and Chapelle et al. [36] have conducted a similar study for metal wires in a polymer matrix.

3. Modeling and governing equations

The present study investigates steady-state conductive heat transfer in a cylindrical composite laminate in which the fibers in each layer are wound in a specific direction. Fig. 1 shows the cylindrical laminate considered in this study. In this figure, r, φ, and z are the coordinates of the off-axis coordinate system (i.e., the reference coordinate system). θ is the angle between the tangent in the fiber direction (N) and the tangent of the cylinder in the φ direction (M).

In the off-axis coordinate system, the Fourier relation for an orthotropic material in a cylindrical coordinate system is given by

$$\begin{Bmatrix} q_r \\ q_\varphi \\ q_z \end{Bmatrix} = -\begin{bmatrix} \bar{k}_{11} & \bar{k}_{12} & \bar{k}_{13} \\ \bar{k}_{21} & \bar{k}_{22} & \bar{k}_{23} \\ \bar{k}_{31} & \bar{k}_{32} & \bar{k}_{33} \end{bmatrix} \begin{Bmatrix} \frac{\partial T}{\partial r} \\ \frac{1}{r}\frac{\partial T}{\partial \varphi} \\ \frac{\partial T}{\partial z} \end{Bmatrix}. \quad (7)$$

The conductive heat transfer equation is obtained by considering the energy balance of a cylindrical element, as follows:

$$\bar{k}_{11}\frac{1}{r}\frac{\partial}{\partial r}\left(r\frac{\partial T}{\partial r}\right) + \bar{k}_{22}\frac{1}{r^2}\frac{\partial^2 T}{\partial \varphi^2} + \bar{k}_{33}\frac{\partial^2 T}{\partial z^2} + (\bar{k}_{12}+\bar{k}_{21})\frac{1}{r}\frac{\partial^2 T}{\partial \varphi \partial r} + (\bar{k}_{13}+\bar{k}_{31})\frac{\partial^2 T}{\partial r \partial z} + \frac{k_{13}}{r}\frac{\partial T}{\partial z} + (\bar{k}_{23}+\bar{k}_{32})\frac{1}{r}\frac{\partial^2 T}{\partial \varphi \partial z} = \rho c \frac{\partial T}{\partial t}. \quad (8)$$

where ρ is the density and c_p is the specific heat capacity at constant pressure. The off-axis components of the conductivity tensor are obtained by substituting Eq. (5) into Eq. (4):

$$\begin{aligned} \bar{k}_{11} &= k_{22} \\ \bar{k}_{22} &= m_l^2 k_{11} + n_l^2 k_{22} \\ \bar{k}_{33} &= n_l^2 k_{11} + m_l^2 k_{22} \\ \bar{k}_{12} &= \bar{k}_{21} = 0 \\ \bar{k}_{13} &= \bar{k}_{31} = 0 \\ \bar{k}_{23} &= \bar{k}_{32} = m_l n_l (k_{11} - k_{22}). \end{aligned} \quad (9)$$

In these relations, m_l and n_l represent $\cos\theta$ and $\sin\theta$, respectively. The heat transfer equation for a cylindrical composite laminate is obtained by substituting Eq. (9) into Eq. (8):

$$k_{22}\frac{1}{r}\frac{\partial}{\partial r}\left(r\frac{\partial T}{\partial r}\right) + \left(m_l^2 k_{11} + n_l^2 k_{22}\right)\frac{1}{r^2}\frac{\partial^2 T}{\partial \varphi^2} + \left(n_l^2 k_{11} + m_l^2 k_{22}\right)\frac{\partial^2 T}{\partial z^2} + 2m_l n_l (k_{11} - k_{22})\frac{1}{r}\frac{\partial^2 T}{\partial \varphi \partial z} = \rho c_p \frac{\partial T}{\partial t}. \quad (10)$$

This study considers steady-state conductive heat transfer in the r and z directions. Thus, Eq. (10) can be simplified to

$$\frac{\partial^2 T}{\partial r^2} + \frac{1}{r}\frac{\partial T}{\partial r} + \frac{1}{\mu^2}\frac{\partial^2 T}{\partial z^2} = 0 \quad (11)$$

where μ is given by

$$\mu = \sqrt{\frac{k_{22}}{n_l^2 k_{11} + m_l^2 k_{22}}}. \quad (12)$$

4. Analytical solution for heat conduction for general boundary conditions

In this section, an analytical solution for Eq. (11) is obtained using the Fourier transformation. The general linear boundary conditions are as follows:

$$a_1 T(r,0) + b_1 \frac{\partial T(r,0)}{\partial z} - f_1(r) = 0 \quad (13a)$$

$$a_2 T(r,L) + b_2 \frac{\partial T(r,L)}{\partial z} - f_2(r) = 0 \quad (13b)$$

$$c_1 T(r_0,z) + d_1 \frac{\partial T(r_0,z)}{\partial r} - g_1(z) = 0 \quad (13c)$$

$$c_2 T(r_{n_l},z) + d_2 \frac{\partial T(r_{n_l},z)}{\partial r} - g_2(z) = 0 \quad (13d)$$

where $f_1(r)$, $f_2(r)$, $g_1(z)$, and $g_2(z)$ are arbitrary functions. The constant coefficients a_1, a_2, c_1, and c_2 have the same dimensions as the convection coefficient (i.e., W/m^{2}K), whereas b_1, b_2, d_1, and d_2 have the same dimensions as the conduction coefficient (i.e., W/mK). Fig. 2 shows the layers in a cylindrical laminate. In this figure, $r = r_i$ at the boundary between layers i and $i+1$. Both the temperature

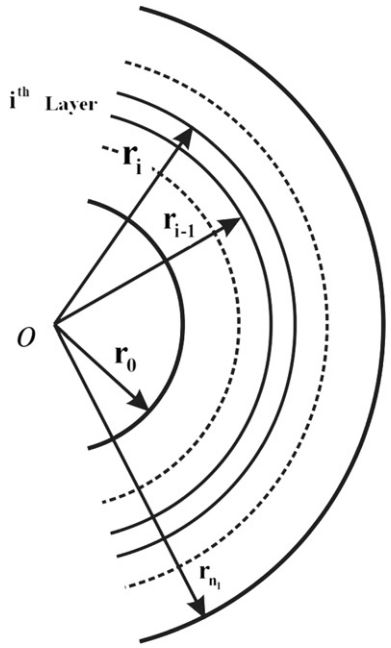

Fig. 2. Arrangement of layers in a cylindrical laminate.

and the heat flux are continuous between the layers (even though the composite material may vary between layers):

$$T^{(i)} - T^{(i+1)} = 0 \tag{13e}$$

$$k_{22}^{(i)}\frac{\partial T^{(i)}}{\partial r} - k_{22}^{(i+1)}\frac{\partial T^{(i+1)}}{\partial r} = 0. \tag{13f}$$

For general boundary conditions, it is necessary to use Sturm–Liouville theory to find a suitable Fourier transformation for the arbitrary function $f(z)$ [37]:

$$F(f) = \frac{\int_a^b s(z)f(z)\phi_n(z)\mathrm{d}z}{\int_a^b s(z)\phi_n^2\mathrm{d}z} \tag{14}$$

where $s(z)$ is the weighting function and $\phi_n(z)$ is the eigenfunction obtained from the solution of the homogeneous equation with homogeneous boundary conditions in the z direction. The inverse Fourier transformation is defined as

$$f(z) = \sum_{n=0}^{\infty} F(f)\phi_n(z). \tag{15}$$

Using the separation of variables method to solve Eq. (11) and applying homogeneous boundary conditions, the following equations in the z direction are obtained:

$$\frac{\partial^2 Z(z)}{\partial z^2} + \lambda^2 Z(z) = 0 \tag{16}$$

$$a_1 Z(0) + b_1\frac{\partial Z(0)}{\partial z} = 0 \tag{17a}$$

$$a_2 Z(L) + b_2\frac{\partial Z(L)}{\partial z} = 0. \tag{17b}$$

The eigenfunction of this problem is obtained by solving Eq. (16) for the boundary conditions given in Eq. (17):

$$\phi_n = (a_1\sin(\lambda_n z) - b_1\lambda_n\cos(\lambda_n z)). \tag{18}$$

By applying the boundary conditions in the z direction (Eq. (17)), the following trigonometric equation is obtained for the eigenvalues:

$$(a_1 b_2 - a_2 b_1)\lambda_n\cos(\lambda_n L) + \left(a_2 a_1 + b_1 b_2\lambda_n^2\right)\sin(\lambda_n L) = 0 \tag{19}$$

The weighting function is constant based on Sturm–Liouville theory and homogeneous boundary conditions in the z direction. A suitable Fourier transformation for this problem is obtained (F) by substituting these relations into the Sturm–Liouville equation (14):

$$F(f) = \frac{4\lambda_n}{A_n^2}\int_0^L [f(z)(a_1\sin(\lambda_n z) - b_1\lambda_n\cos(\lambda_n z))]\mathrm{d}z \tag{20}$$

where

$$A_n = \sqrt{\left(-a_1^2 + (b_1\lambda_n)^2\right)\sin(2\lambda_n L) + 2a_1 b_1\lambda_n\cos(2\lambda_n L) + 2\lambda_n\left(a_1^2 + (b_1\lambda_n)^2\right)L - 2a_1 b_1\lambda_n}. \tag{21}$$

From the definition of the Fourier transformation, the second derivative with respect to z is given by

$$F(f'') = \left\{\left(\frac{2\lambda_n}{A_n}\right)^2\left[\frac{-a_1}{(a_2\cos(\lambda_n L) - b_2\lambda_n\sin(\lambda_n L))}f_2(r) + f_1(r)\right] - \lambda_n^2 F(f)\right\}. \tag{22}$$

The following relations are obtained by applying this Fourier transformation to Eq. (11) and the boundary conditions in the r direction (Eqs. (13c) and (13d)):

$$\frac{\partial^2 U}{\partial r^2} + \frac{1}{r}\frac{\partial U}{\partial r} - \left(\frac{\lambda_n^2}{\mu}\right)^2 U = \left(\frac{2\lambda_n^2}{A_n^2\mu}\right)^2 \times\left[\frac{a_1}{(a_2\cos(\lambda_n L) - b_2\lambda_n\sin(\lambda_n z))}f_2(r) - f_1(r)\right] \tag{23}$$

$$c_1 U(r_0, n) + d_1\frac{\partial U(r_0, n)}{\partial r} - G_1(n) = 0 \tag{24a}$$

$$c_2 U(r_{n_l}, n) + d_2\frac{\partial U(r_{n_l}, n)}{\partial r} - G_2(n) = 0 \tag{24b}$$

where

$$U(r, n) = F(T(r, z)) \tag{25a}$$

$$G_1(n) = F(g_1(z)) \tag{25b}$$

$$G_2(n) = F(g_2(z)). \tag{25c}$$

If the right-hand side of Eq. (23) is equal to $h(r,n)$, the general solution of this equation in each composite lamina will be

$$U^{(i)}(r,n) = a_n^{(i)} I_0\left(\frac{\lambda_n}{\mu_i}r\right) + b_n^{(i)} K_0\left(\frac{\lambda_n}{\mu_i}r\right) + w^{(i)}(r,n) \tag{26}$$

where $w(r,n)$ is the non-homogeneous solution for Eq. (23). Its general form is given by

$$w^{(i)}(r,n) = I_0\left(\frac{\lambda_n}{\mu_i}r\right) \times \int_{r_{in}}^{r_{out}} \left[r \times K_0\left(\frac{\lambda_n}{\mu_i}r\right) \times h(r,n)\right] dr + K_0\left(\frac{\lambda_n}{\mu_i}r\right) \times \int_{r_{in}}^{r_{out}} \left[r \times I_0\left(\frac{\lambda_n}{\mu_i}r\right) \times h(r,n)\right] dr \tag{27}$$

where I_0 and K_0 are respectively modified Bessel functions of the first and second kinds of order zero. Finally, by applying the inner and outer boundary conditions in the direction of r and applying the continuity of temperature and heat flux at the boundary between layers, the coefficients a_n and b_n are obtained. Thus, according to Eq. (24a) we have

$$a_n^{(1)}\left[c_1 I_0\left(\frac{\lambda_n}{\mu_1}r_0\right) + d_1\frac{\lambda_n}{\mu_1} I_1\left(\frac{\lambda_n}{\mu_1}r_0\right)\right] + b_n^{(1)}\left[c_1 K_0\left(\frac{\lambda_n}{\mu_1}r_0\right) - d_1\frac{\lambda_n}{\mu_1} K_1\left(\frac{\lambda_n}{\mu_1}r_0\right)\right] = G_1(n) - w^{(1)}(r_0,n). \tag{28a}$$

Similarly, for the boundary conditions of Eq. (24b):

$$a_n^{(n_l)}\left[c_2 I_0\left(\frac{\lambda_n}{\mu_{n_l}}r_{n_l}\right) + d_2\frac{\lambda_n}{\mu_{n_l}} I_1\left(\frac{\lambda_n}{\mu_{n_l}}r_{n_l}\right)\right] + b_n^{(n_l)}\left[c_2 K_0\left(\frac{\lambda_n}{\mu_{n_l}}r_{n_l}\right) - d_2\frac{\lambda_n}{\mu_{n_l}} K_1\left(\frac{\lambda_n}{\mu_{n_l}}r_{n_l}\right)\right] = G_1(n) - w^{(n_l)}(r_{n_l},n). \tag{28b}$$

From temperature continuity (Eq. (13e)), we have

$$U^{(i)}(r_0,n) = U^{(i+1)}(r_0,n) \Rightarrow a_n^{(i)} I_0\left(\frac{\lambda_n}{\mu_i}r_i\right) + b_n^{(i)} K_0\left(\frac{\lambda_n}{\mu_i}r_i\right) - a_n^{(i+1)} I_0\left(\frac{\lambda_n}{\mu_{i+1}}r_i\right) + b_n^{(i+1)} K_0\left(\frac{\lambda_n}{\mu_{i+1}}r_i\right) = w^{(i+1)}(r_i,n) - w^{(i)}(r_i,n). \tag{28c}$$

From Eq. (13f), which expresses heat flux continuity, the following relation is obtained:

$$k_{22}^{(i)}\frac{\partial U^{(i)}(r_0,n)}{\partial r} = k_{22}^{(i+1)}\frac{\partial U^{(i+1)}(r_0,n)}{\partial r} \Rightarrow k_{22}^{(i)}\left[a_n^{(i)}\frac{\lambda_n}{\mu_i} I_1\left(\frac{\lambda_n}{\mu_i}r_i\right) + b_n^{(i)}\frac{\lambda_n}{\mu_i} K_1\left(\frac{\lambda_n}{\mu_i}r_i\right)\right] - k_{22}^{(i+1)}\left[a_n^{(i+1)}\frac{\lambda_n}{\mu_{i+1}} I_1\left(\frac{\lambda_n}{\mu_{i+1}}r_i\right) + b_n^{(i+1)}\frac{\lambda_n}{\mu_{i+1}} K_1\left(\frac{\lambda_n}{\mu_{i+1}}r_i\right)\right] = k_{22}^{(i+1)}\frac{\partial w^{(i+1)}(r_i,n)}{\partial r} - k_{22}^{(i)}\frac{\partial w^{(i)}(r_i,n)}{\partial r} \tag{28d}$$

where I_1 and K_1 are respectively modified Bessel functions of the first and second kinds of order one. Equations (28a)–(28d) are solved to determine the coefficients $a_n^{(i)}$ and $b_n^{(i)}$. The coefficients of this set of equations form a five diagonal matrix. In this study, this five diagonal matrix is converted into a two diagonal matrix using the Thomas algorithm. The diametric elements of this matrix are unity. Based on this algorithm, the reciprocity relations for calculating a_n and b_n are given by:

$$a_n^{(1)} = M_n^{(1)} \tag{29a}$$

$$\begin{cases} b_n^{(i)} = N_n^{(i)} - \alpha_n^{(i)} a_n^{(i)} \\ a_n^{(i+1)} = M_n^{(i+1)} - \beta_n^{(i+1)} b_n^{(i)} \end{cases} \quad 1 < i < n_l - 1 \tag{29b}$$

$$b_n^{(n_l)} = N_n^{n_l} - \alpha_n^{(n_l)} a_n^{(n_l)}. \tag{29c}$$

The parameters α_n, β_n, N_n, and M_n in these relations are obtained for all layers from the following relations:

$$\alpha_n^{(n_l)} = \frac{c_2 I_0\left(\frac{\lambda_n}{\mu_{n_l}}r_{n_l}\right) + d_2\frac{\lambda_n}{\mu_{n_l}} I_1\left(\frac{\lambda_n}{\mu_{n_l}}r_{n_l}\right)}{c_2 K_0\left(\frac{\lambda_n}{\mu_{n_l}}r_{n_l}\right) - d_2\frac{\lambda_n}{\mu_{n_l}} K_1\left(\frac{\lambda_n}{\mu_{n_l}}r_{n_l}\right)} \tag{30a}$$

$$N_n^{(n_l)} = \frac{G_2(n) - w^{(n_l)}(r_{n_l},n)}{c_2 K_0\left(\frac{\lambda_n}{\mu_{n_l}}r_{n_l}\right) - d_2\frac{\lambda_n}{\mu_{n_l}} K_1\left(\frac{\lambda_n}{\mu_{n_l}}r_{n_l}\right)} \tag{30b}$$

$$\begin{cases} \beta_n^{(i+1)} = \dfrac{\pi_i}{\chi_i - \alpha_n^{(i+1)}} \\ M_n^{(i+1)} = \dfrac{E_i - N_n^{(i+1)}}{\chi_i - \alpha_n^{(i+1)}} \\ \alpha_n^{(i)} = \dfrac{\gamma_i}{\psi_i - \beta_n^{(i+1)}} \\ N_n^{(i)} = \dfrac{F_i - M_n^{(i+1)}}{\psi_i - \beta_n^{(i+1)}} \end{cases} \quad 1 < i < n_l - 1 \tag{30c}$$

$$M_n^{(1)} = \frac{G_1(n) - w^{(1)}(r_0,n) - N_n^{(1)}\left(c_1 k_0\left(\frac{\lambda_n}{\mu_1}r_0\right) - d_1\frac{\lambda_n}{\mu_1} K_1\left(\frac{\lambda_n}{\mu_1}r_0\right)\right)}{\left(c_1 I_0\left(\frac{\lambda_n}{\mu_1}r_0\right) + d_1\frac{\lambda_n}{\mu_1} I_1\left(\frac{\lambda_n}{\mu_1}r_0\right)\right) - \alpha_n^{(1)}\left(c_1 k_0\left(\frac{\lambda_n}{\mu_1}r_0\right) - d_1\frac{\lambda_n}{\mu_1} K_1\left(\frac{\lambda_n}{\mu_1}r_0\right)\right)} \tag{30d}$$

where the constant coefficients π_i, χ_i, γ_i, ψ_i, E_i, and F_i are given by:

Table 1
Properties of graphite/epoxy composite material [38].

k in parallel direction of fibers (W/mK)	11.1
k in perpendicular direction of fibers (W/mK)	0.87
Volumetric percentage of fibers	75
Melting point (K)	450
Heat capacity (J/kg K)	935
Density (kg/m^3)	1400

$$\pi_i = \frac{-I_0\left(\frac{\lambda_n}{\mu_i}r_i\right)K_1\left(\frac{\lambda_n}{\mu_i}r_i\right) - I_1\left(\frac{\lambda_n}{\mu_i}r_i\right)K_0\left(\frac{\lambda_n}{\mu_i}r_i\right)}{\frac{\mu_i}{\mu_{i+1}}\frac{k_{22}^{(i+1)}}{k_{22}^{(i)}}I_0\left(\frac{\lambda_n}{\mu_i}r_i\right)K_1\left(\frac{\lambda_n}{\mu_{i+1}}r_i\right) + I_1\left(\frac{\lambda_n}{\mu_i}r_i\right)K_0\left(\frac{\lambda_n}{\mu_{i+1}}r_i\right)} \tag{31a}$$

$$\chi_i = \frac{-\frac{\mu_i}{\mu_{i+1}}\frac{k_{22}^{(i+1)}}{k_{22}^{(i)}}I_0\left(\frac{\lambda_n}{\mu_i}r_i\right)I_1\left(\frac{\lambda_n}{\mu_{i+1}}r_i\right) + I_0\left(\frac{\lambda_n}{\mu_{i+1}}r_i\right)I_1\left(\frac{\lambda_n}{\mu_i}r_i\right)}{\frac{\mu_i}{\mu_{i+1}}\frac{k_{22}^{(i+1)}}{k_{22}^{(i)}}I_0\left(\frac{\lambda_n}{\mu_i}r_i\right)K_1\left(\frac{\lambda_n}{\mu_{i+1}}r_i\right) + I_1\left(\frac{\lambda_n}{\mu_i}r_i\right)K_0\left(\frac{\lambda_n}{\mu_{i+1}}r_i\right)} \tag{31b}$$

$$\gamma_i = \frac{I_0\left(\frac{\lambda_n}{\mu_i}r_i\right)}{\chi_i \times K_0\left(\frac{\lambda_n}{\mu_{i+1}}r_i\right) - I_0\left(\frac{\lambda_n}{\mu_{i+1}}r_i\right)} \tag{31c}$$

$$\psi_i = \frac{\pi_i \times K_0\left(\frac{\lambda_n}{\mu_{i+1}}r_i\right) + K_0\left(\frac{\lambda_n}{\mu_i}r_i\right)}{\chi_i \times K_0\left(\frac{\lambda_n}{\mu_{i+1}}r_i\right) - I_0\left(\frac{\lambda_n}{\mu_{i+1}}r_i\right)} \tag{31d}$$

$$E_i = \pi_i\left[\left(k_{22}^{(i+1)}\frac{\partial w^{(i+1)}(r_i,n)}{\partial r} - k_{22}^{(i)}\frac{\partial w^{(i)}(r_i,n)}{\partial r}\right) - \frac{\lambda_n}{\mu_i}k_{22}^{(i)}\left(w^{(i+1)}(r_i,n) - w^{(i)}(r_i,n)\right)I_1\left(\frac{\lambda_n}{\mu_{i+1}}r_i\right)\right] \tag{31e}$$

$$F_i = \frac{E_i \times K_0\left(\frac{\lambda_n}{\mu_{i+1}}r_i\right) - w^{(i+1)}(r_i,n) - w^{(i)}(r_i,n)}{\chi_i \times K_0\left(\frac{\lambda_n}{\mu_{i+1}}r_i\right) - I_0\left(\frac{\lambda_n}{\mu_{i+1}}r_i\right)}. \tag{31f}$$

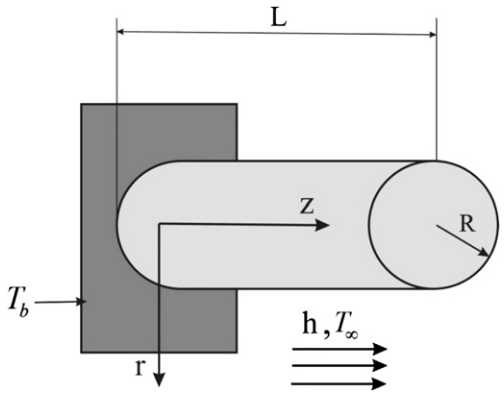

Fig. 3. Geometry of the solid pin fin.

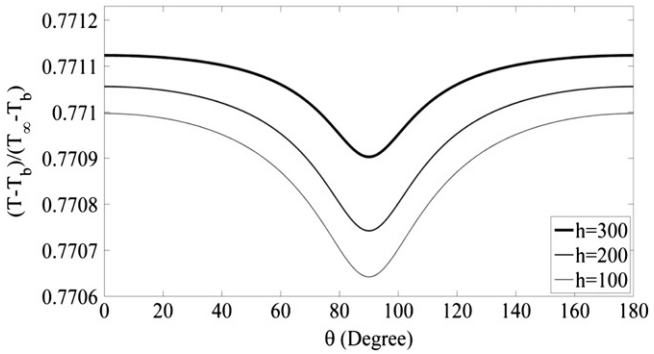

Fig. 4. Mean dimensionless temperature in term of the fibers angle under the different convective coefficients ($k_{11} = 11.4$ *W/m.K*, $k_{22} = 0.74$ *W/m.K*, $L = 7cm$).

For solid cylinders, the following modification for the first layer must be implemented. It is based on the axisymmetry $((\partial T/\partial r) = 0)$ about the cylinder axis. Equation (30d) should be changed to

$$M_n^{(1)} = \frac{N_n^{(1)}}{\alpha_n^{(1)}}. \tag{32}$$

This change gives $b_n^{(1)} = 0$, so it is necessary to modify Eq. (29) to

$$\begin{cases} a_n^{(1)} = M_n^{(1)} \\ b_n^{(1)} = 0 \end{cases} \tag{33a}$$

$$\begin{cases} b_n^{(i)} = N_n^{(i)} - \alpha_n^{(i)}a_n^{(i)} \\ a_n^{(i)} = M_n^{(i)} - \beta_n^{(i)}b_n^{(i)} \end{cases} \quad 2 < i < n_l - 1 \tag{33b}$$

$$b_n^{(n_l)} = N_n^{n_l} - \alpha_n^{(n_l)}a_n^{(n_l)}. \tag{33c}$$

Finally, the temperature distribution in each layer is determined by applying the inverse Fourier transformation (Eq. (15)) to Eq. (26):

$$\begin{aligned} T^{(i)}(r,z) &= \sum_{n=1}^{\infty}\left(U^{(i)}(r,n) \times \phi_n(z)\right) \\ &= \sum_{n=1}^{\infty}\left(a_n^{(i)}I_0\left(\frac{\lambda_n}{\mu_i}r\right) + b_n^{(i)}K_0\left(\frac{\lambda_n}{\mu_i}r\right) + w^{(i)}(r,n)\right) \\ &\quad \times (a_1\sin(\lambda_n z) - b_1\lambda_n\cos(\lambda_n z)). \end{aligned} \tag{34}$$

5. Results and discussion

In this section, the validity of the current solution is demonstrated by applying it to two examples of industrial applications: a multilayer pin fin (treated as a solid cylinder) and a multilayer composite coolant pipe with a longitudinally varying heat flux. A graphite/epoxy composite was used to investigate thermal conduction in a composite material. Graphite fibers and epoxy have conductive heat transfer coefficients of 14.74 and 0.19 W/mK,

Table 2
Geometry and boundary conditions of fin.

Outer diameter (cm)	1
Length (cm)	10
Thickness of each layer (cm)	0.1
Ambient temperature (K)	320
Base temperature (K)	370
Convective coefficient (W/m^{2}K)	100

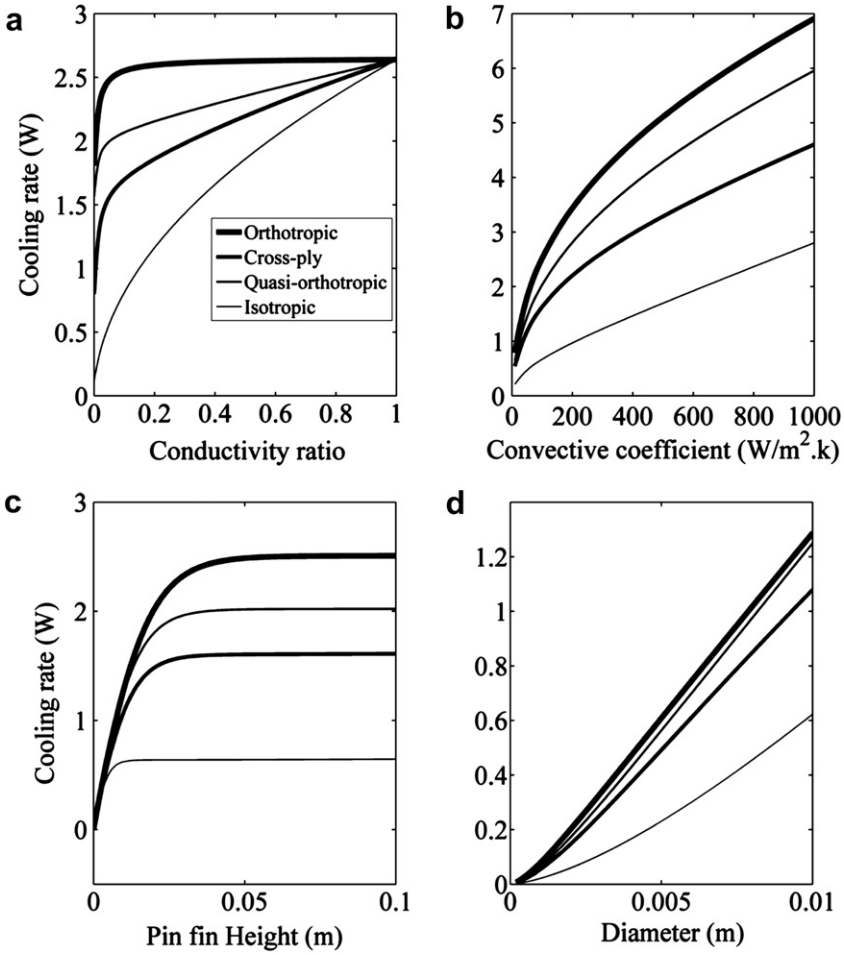

Fig. 5. Composite pin fin cooling rate variation versus (a) conductivity ratio, (b) convective coefficient, (c) pin fin height, (d) pin fin diameter.

respectively [38]. The conductive coefficients of the graphite fibers and the epoxy matrix differ greatly. Consequently, the thermal conductivity of this composite laminate parallel to the fibers is much greater than that perpendicular to the fibers. Table 1 lists the properties of graphite/epoxy laminate for a fiber volume percentage of 75.

5.1. Pin fin

This section considers heat conduction in a five-layer pin fin for various laminate structures. Fig. 3 shows the geometry of the solid pin fin together with the coordinate system used. Table 2 lists the geometric parameters and the boundary conditions of the pin fin.

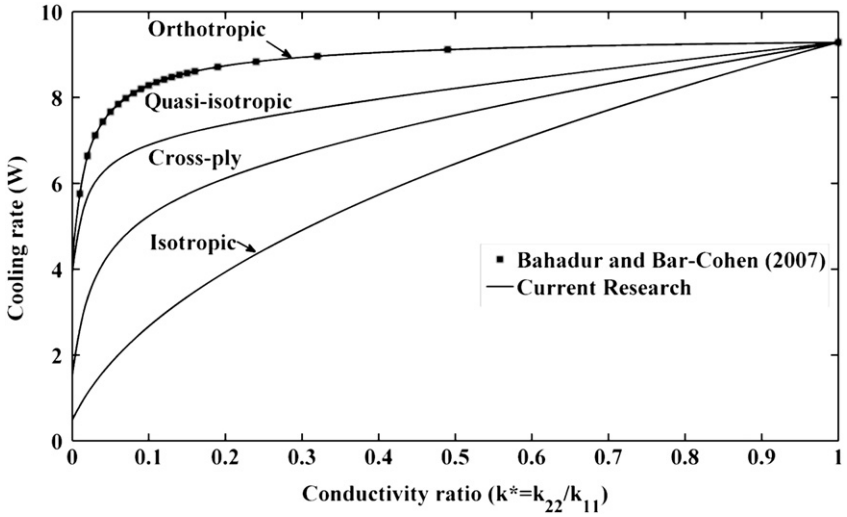

Fig. 6. Composite pin fin cooling rate variation with conductivity ratio.

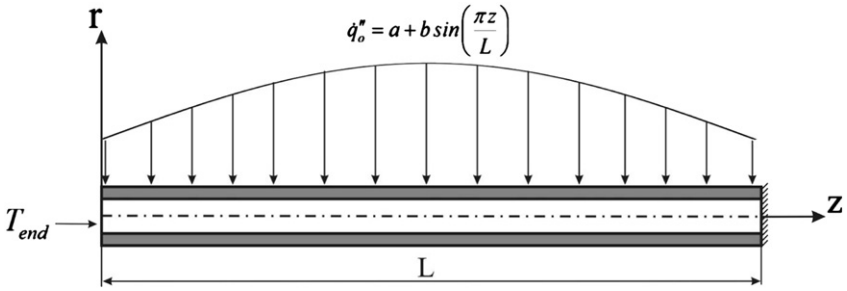

Fig. 7. Geometry of the cooling pipe.

The pin fin is assumed to have a constant temperature at its base and to be thermally isolated at its end. The outer surface of the pin fin is cooled by air.

A single-layer pin fin (which is equivalent to a multilayered pin fin with equal fiber angles in all its layers) was used to investigate the effect of varying the fiber angle on the temperature distribution. The following relative temperature is defined:

$$T^* = (T - T_b)/(T_\infty - T_b) \tag{35}$$

where T_b and T_∞ are the base and ambient temperatures, respectively. Fig. 4 shows the variations in the mean relative temperature with fiber angle for different values of the convection coefficient (h). The conduction coefficient in the z direction increases as the fiber angle approaches 90°. This will reduce the temperature gradient in the laminate and consequently the mean dimensionless temperature will decrease. If the fiber angle is 0°, the fibers will be aligned with the φ direction and the heat transfer will be similar to that in an isotropic cylinder with conduction coefficients $k_{rr} = k_{zz} = k_{22}$. On the other hand, when the fiber angle is 90°, the fibers will be aligned with the z direction and the heat transfer will be similar to that in an orthotropic cylinder with conduction coefficients $k_{zz} = k_{11}$ and $k_{rr} = k_{22}$. Two common laminate structures, cross-ply [0°,90°,0°,90°,0°] and quasi-isotropic [0°,45°,90°,135°,180°], were considered in this study. Fig. 4 shows that single-layer laminates with fiber angles of 0° and 90° have the maximum and minimum temperature distributions, respectively. Thus, other fiber arrangements will have intermediate temperature distributions between these two cases.

The effect of varying different parameters on the pin fin cooling rate was investigated to compare different laminate structures. The term of cooling rate shows the total heat transfer through the fin. Fig. 5a shows the variations of pin fin cooling rate as a function of the conductivity ratio ($k^* = k_{11}/k_{22}$) for a constant conduction coefficient $k_{11} = 11.1$ W/mK for four fiber arrangements. The cooling rate increases with increasing conductivity ratio. A single-layer laminate with $\theta = 90°$ has the highest cooling rate through the pin fin. The variation in the cooling rate is negligible for $k^* \geq 0.1$.

Fig. 5b shows variation in the cooling rate as a function of the thermal convection coefficient (h) for different fiber arrangements. The cooling rate increases greatly as the thermal convection coefficient increases. Fig. 5c depicts the variation in the cooling rate of the pin fin as a function of the pin height for different fiber arrangements. There is negligible variation in the cooling rate for $L \geq 0.05$ m for all the arrangements. Fig. 5d shows the variation in the cooling rate with pin fin diameter; the cooling rate increases steeply with increasing diameter.

Bahadur and Bar-Cohen have investigated heat conduction in a single-layer orthotropic pin fin [16]. They developed an analytical solution for this problem and investigated the effect of the same parameter on the pin fin. To confirm the validity of the present results, we plotted the cooling rate as a function of the conductivity ratio for $L = 5$ cm, $D = 0.9$ cm, and $k_{11} = 20$ W/mK (see Fig. 6). As Fig. 6 shows, the result for the orthotropic case agrees completely with the solution of Bahadur and Bar-Cohen [16].

Table 3
Geometry and boundary conditions of cooling pipe.

Outer diameter (cm)	3
Length (cm)	1.22
Thickness of each layer (cm)	0.3
Ambient temperature (°C)	250
Internal mean temperature (°C)	280
End temperature (°C)	100
Convective coefficient (W/m^{2}K)	50

5.2. Nuclear reactor cooling pipe

This section considers another example of an application to investigate the effects of a longitudinally varying heat flux on the temperature distributions in cylindrical composite laminates. The following relation is used to describe the variation in the heat flux with length for a nuclear reactor cooling pipe [39].

$$\dot{q}''_o = a + b\sin\left(\frac{\pi z}{L}\right) \tag{36}$$

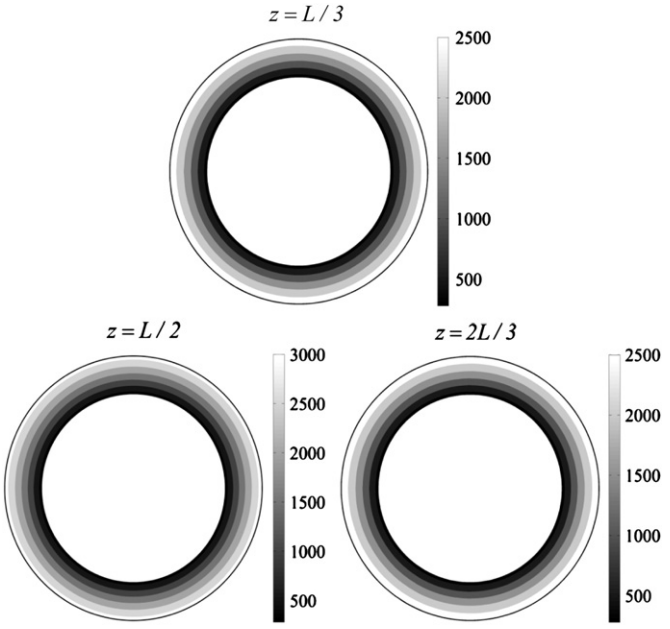

Fig. 8. Contours for steady state temperature distribution in radial direction for the different longitudinal cross sections in the case of single layer laminate at $\theta = 90°$.

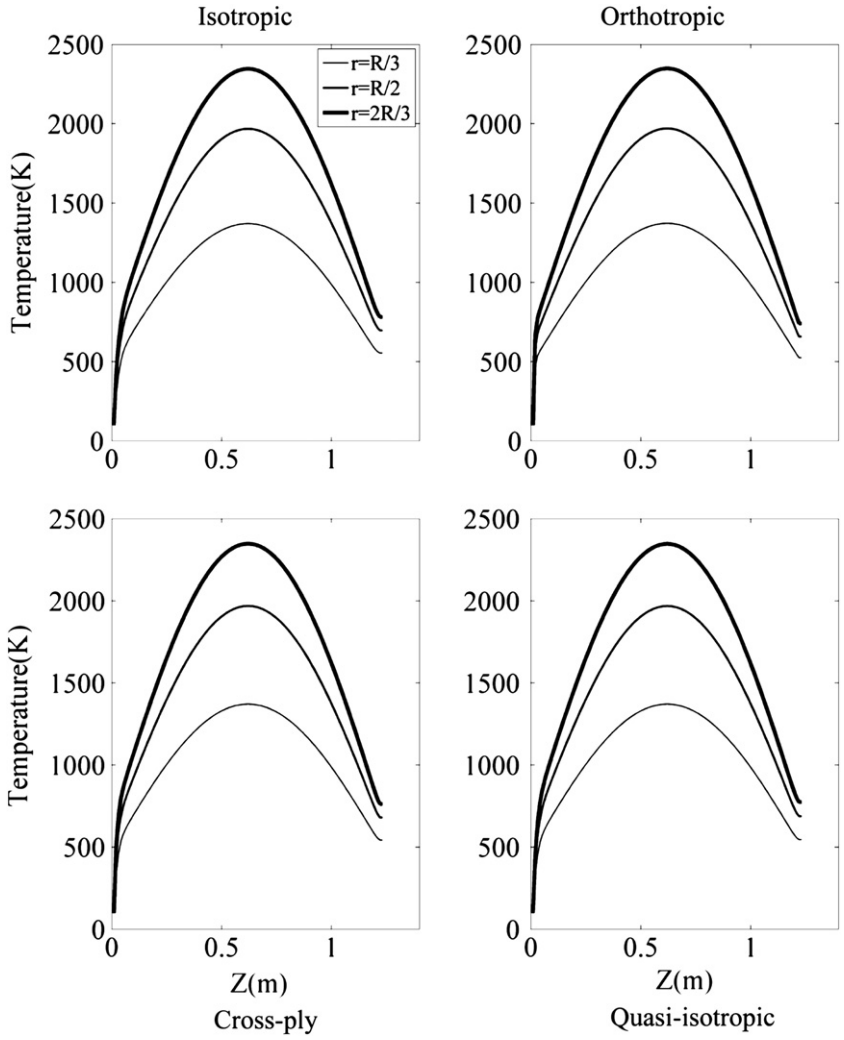

Fig. 9. Contours of steady state temperature distribution in the different radial cross sections for the different arrangement of laminates.

where L is the length and x is the longitudinal distance along the pipe. We consider a four-layer graphite/epoxy composite pipe. Fig. 7 shows the geometry and the boundary conditions of the pipe, and Table 3 lists its properties. In Eq. (36), a and b are respectively set to 900 and 2500 W/m^2. The temperature is constant on the left-hand side of the pipe while the right-hand side is thermally isolated. The outer surface of the reactor is assumed to be cooled with air and the heat flux on the outer surface is assumed to vary longitudinally (as Eq. (36)). We also assume that convection occurs inside the pipe.

As mentioned in the previous section, when the fibers in all the layers are orientated at 90°, the temperature distribution is similar to that in an orthotropic medium. Fig. 8 shows temperature contour plots of laminates with various longitudinal cross-sections. This figure shows that the temperature distribution is approximately linear in the r direction.

Fig. 9 shows the temperature distribution in the longitudinal direction for different radial sections. This figure depicts four different fiber arrangements like orthotropic, isotropic, cross-ply, and quasi-isotropic. Due to the cylinder length being greater than its radius, the temperature distribution in the z direction does not vary significantly for the different fiber arrangements, but it has a clear variation in the r direction.

6. Conclusion

The present investigation developed an exact analytical solution for steady-state heat conduction for general boundary conditions. The main findings of this study are as follows:

- Because general boundary conditions were employed, the present analytical solution can be used for a wide range of thermal boundary conditions, which includes many applied problems.
- The temperature distribution in a composite laminate with an arbitrary fiber arrangement will be intermediate between those in single-layer laminates with fiber angles of $\theta = 0°$ and $\theta = 90°$.
- For a pin fin, the highest cooling rate is obtained when the fiber angles in all layers are $\theta = 90°$.
- For a cooling pipe, the temperature distribution is quasilinear when the fiber angle is $\theta = 90°$.

References

[1] C.K. Chao, F.M. Che, M.H. Shen, An exact solution for thermal stresses in a three-phase composite cylinder under uniform heat flow, Int. J. Solids Struct. 44 (2007) 926–940.

[2] V. Pradeep, N. Ganesan, Thermal buckling and vibration behavior of multilayer rectangular viscoelastic sandwich plates, J. Sound Vibrat. 310 (2008) 169–183.
[3] J.Q. Tarn, State space formalism for anisotropic elasticity, Part II: cylindrical anisotropy, Int. J. Solids Struct. 39 (2002) 5157–5172.
[4] W.A. Wooster, A Textbook in Crystal Physics, Cambridge University Press, London, p. 455.
[5] J.F. Nye, Physical Properties of Crystals. Clarendon Press, London, 1957, p. 957.
[6] C.C. Ma, S.S. Chang, Analytical exact solutions of heat conduction problems for anisotropic multilayered media, Int. J. Heat Mass Transfer 47 (2004) 1643–1655.
[7] Y.S. Cha, W.J. Minkowycz, S.Y. Seol, Transverse temperature distribution and heat generation rate in composite superconductors subjected to constant thermal disturbance, Int. Commun. Heat Mass Transfer 22 (4) (1995) 461–474.
[8] M.R. Kulkarani, R.P. Brady, A model of global thermal conductivity in laminated Carboncarbon composites, Compos. Sci. Technol. 57 (1997) 277–285.
[9] B.T. Johansson, D. Lesnic, A method of fundamental solutions for transient heat conduction in layered materials, Eng. Anal. Boundary Elements 33 (2009) 1362–1367.
[10] G. Fairweather, A. Karageorghis, The method of fundamental solutions for elliptic boundary value problems, Advan. Comput. Math. 9 (1998) 69–95.
[11] Y. Sun, I.S. Wichman, On transient heat conduction in a one-dimensional composite slab, Int. J. Heat Mass Transfer 47 (2004) 1555–1559.
[12] A. Karageorghis, D. Lesnic, Steady-state nonlinear heat conduction in composite materials, Comput. Methods Appl. Mech. Eng. 197 (2008) 3122–3137.
[13] A. Haji-Sheikh, J.V. Beck, D. Agonater, Steady-state heat conduction in multilayer bodies, Int. J. Heat Mass Transfer 46 (2003) 2363–2379.
[14] Z.S. Guo, S.Y. Du, B.M. Zhang, Temperature distribution of thick thermo set composites, Model. Simulat. Mater. Sci. Eng. 12 (3) (2004) 443–452.
[15] S. Singh, P.K. Jain, Rizwan-uddin, Analytical solution to transient heat conduction in polar coordinates with multiple layers in radial direction, Int. J. Thermal Sci. 47 (2008) 261–273.
[16] R. Bahadur, A. Bar-Cohen, Orthotropic thermal conductivity effect on cylindrical pin fin heat transfer, Int. J. Heat Mass Transfer 50 (2007) 1155–1162.
[17] O.O. Onyejekwe, Heat conduction in composite media: a boundary integral approach, Comput. Chem. Eng. 26 (2002) 1621–1632.
[18] J.Q. Tarn, Y.M. Wang, Heat conduction in a cylindrically anisotropic tube of a functionally graded material, Chin J. Mech. 19 (2003) 365–372.
[19] J.Q. Tarn, Y.M. Wang, End effects of heat conduction in circular cylinders of functionally graded materials and laminated composites, Int. J. Heat Mass Transfer 47 (2004) 5741–5747.
[20] J. Zhang, M. Tanaka, T. Matsumoto, A simplified approach for heat conduction analysis of CNT-based nano-composites, Comput. Methods Appl. Mech. Eng. 193 (2004) 5597–5609.
[21] N.A. Roberts, D.G. Walker, D.Y. Li, Molecular dynamics simulation of thermal conductivity of nanocrystalline composite films, Int. J. Heat Mass Transfer 52 (2008) 2002–2008.
[22] M.H. Kayhani, M. Shariati, M. Norouzi, M. Karimi Demneh, Exact solution of conductive heat transfer in cylindrical composite laminate, Heat Mass Transfer 46 (2009) 83–94 Waerme- und Stoffuebertragung from Springer Verlag.
[23] M.H. Kayhani, M. Norouzi, A.A. Delouei, An exact solution of axi-symmetric conductive heat transfer in cylindrical composite laminate under the general boundary condition, Word Acad. Sci. Eng. Technol. 69 (2010) 55–62.
[24] M.N. Ozisik, Heat Conduction. Wiley, New York, 1993.
[25] Y. Fung, Foundation of Solid Mechanics. Prentice-Hall, Englewood Cliffs, 1965.
[26] J.M. Powers, On the necessity of positive semi-definite conductivity and Onsager reciprocity in modeling heat conduction in anisotropic media, J. Heat Transfer Trans. ASME 126 (2004) 670–675.
[27] C.T. Herakovich, Mechanics of Fibrous Composites. Wiley, New York, 1998.
[28] J.C. Halpin, Primer on Composite Materials Analysis. CRC Press, Boca Raton, 1992.
[29] J.C. Maxwell, A Treatise on Electricity and Magnetism, third ed. Dover Publications, New York, 1954.
[30] D.A.G. Bruggeman, Calculation of various physical constants in heterogeneous substances. I. Dielectric constants and conductivity of composites from isotropic substances (German), Ann. Phys. 24 (1935) 636–679.
[31] S. Torquato, Bulk properties of two-phase disordered media. I. Cluster expansion for the effective dielectric constant of dispersions of penetrable spheres, J. Chem. Phys. 81 (1984) 5079–5088.
[32] Z. Hashin, S. Shtrikman, A variational approach to the theory of the effective magnetic permeability of multiphase materials, J. Appl. Phys. 33 (1962) 1514–1517.
[33] T.B. Lewis, L.E. Nielsen, Dynamic mechanical properties of particulate-filled polymers, J. Appl. Polym. Sci. 14 (1970) 1449–1471.
[34] D.P.H. Hasselman, K.Y. Donaldson, J.R. Thomas, Effective thermal conductivity of uniaxial composite with cylindrically orthotropic carbon fibers and interfacial thermal barrier, J. Compos. Mater. 27 (1993) 637–644.
[35] F. Macedo, J.A. Ferreira, Thermal contact resistance evaluation in polymer-based carbon fiber, Rev. Sci. Instrum. 74 (2003) 828–830.
[36] E. Chapelle, B. Garnier, B. Bourouga, Interfacial thermal resistance measurement between metallic wire and polymer in polymer matrix composites, Int. J. Thermal Sci. 48 (2009) 2221–2227.
[37] T. Myint-U, L. Debnath, Linear Partial Differential Equations for Scientists and Engineers. Birkhauser Boston, 2007.
[38] Y.S. Touloukian, C.Y. Ho, Thermo physical properties of matter, , In: Thermal Conductivity of Nonmetallic Solids, vol. 2. Plenum Press, New York, 1972.
[39] W.M. Kays, M.E. Crawford, B. Weigand, Convective Heat and Mass Transfer, fourth ed. McGraw-Hill, 2005.